CANCER GENOMICS & PROTEOMICS *12*: 133-142 (2015)

Effect of STAT3 Inhibition on the Metabolic Switch in a Highly STAT3-activated Lymphoma Cell Line

YASUTO AKIYAMA[1*], AKIRA IIZUKA[1*], AKIKO KUME[1], MASARU KOMIYAMA[1], KENICHI URAKAMI[2], TADASHI ASHIZAWA[1], HARUO MIYATA[1], MAHO OMIYA[1], MASATOSHI KUSUHARA[3] and KEN YAMAGUCHI[4]

[1]Immunotherapy Division, [2]Cancer Diagnostics Division, [3]Regional Resources Division, Shizuoka Cancer Center Research Institute, Sunto-gun, Shizuoka, Japan; [4]Office of the President, Shizuoka Cancer Center Hospital, Sunto-gun, Shizuoka, Japan

Abstract. *Background: Signal transducer and activator of transcription (STAT)3 is involved in a metabolic shift in cancer cells, the Warburg effect through its pro-oncogenic activity. To develop efficient STAT3 inhibitors against cancer cells, novel proteomic and metabolic target molecules need to be explored using multi-omics approaches in the context of STAT3 gene inhibition-mediated tumor growth suppression. Materials and Methods: We found that short hairpin (sh)RNA-mediated STAT3 inhibition suppressed tumor growth in a highly STAT3-activated lymphoma cell line, SCC-3 cells, and we investigated the effect of STAT3 inhibition on metabolic switching using 2-dimensional differential gel electrophoresis and capillary electrophoresis-time of flight-mass spectrometry. Results: We identified latexin as a proteomic marker candidate and metabolic enzymes including fructose-bisphosphate aldolase A (ALDOA) as a metabolic marker candidate for STAT3-targeting therapy using STAT3-specific shRNA gene transduction. In particular, latexin expression was up-regulated in four STAT3-activated cancer cell lines including SCC-3 transduced with STAT3-specific shRNA. The up-regulation of latexin was identified in SCC-3 tumors transplanted to nude mice after treatment with STAT3 inhibitor. Conclusion: Our results suggest that STAT3 inactivation reverses the glycolytic shift by down-regulating key enzymes and that it induces up-regulation of latexin as a tumor-suppressor molecule, which partially results in cancer cell apoptosis and tumor growth suppression.*

The signal transducer and activator of transcription (STAT) protein family is a group of transcription factors that play an important role in relaying signals from growth factors and cytokines. STAT3 is involved in oncogenesis by up-regulating the transcription of several genes that control tumor cell survival, resistance to apoptosis, cell-cycle progression and angiogenesis (1, 2). Targets of STAT3 include BCL-2, BCL-xL, c-MYC, cyclin D1, vascular endothelial growth factor (VEGF), hypoxia-inducible factor (HIF)-1α and human telomerase reverse transcriptase.

Most tumor cells switch their metabolism towards aerobic glycolysis by increasing glycolysis and reducing oxidative phosphorylation even under high-oxygen conditions (3-6). This switch is known as the Warburg effect, which favors rapidly proliferating cells such as cancer cells by promoting the synthesis of essential cellular components, including the nucleotides and lipids needed for fast cell duplication.

Unexpectedly, STAT3 localizes to mitochondria when phosphorylated at serine 727. Moreover, STAT3 mitochondrial localization is required for RAS-dependent oncogenic transformation, which can regulate the metabolic function of a cancer cell by increasing glycolysis and decreasing oxidative phosphorylation (7, 8).

*These Authors contributed equally to this study.

Abbreviations: STAT, Signal transducer and activator of transcription; shRNA, short hairpin RNA; HIF-1α, hypoxia-inducible factor-1α; ALDOA, fructose-bisphosphate aldolase A; glucose-6P, glucose-6-phosphate; fructose-1,6BP, fructose-1,6-bisphosphate; HK2, hexokinase 2; PDK1, pyruvate dehydrogenase kinase 1; PFKFB3, 6-phosphofructo-2-kinase/fructose-2,6-bisphosphatase 3; PFKM, phosphofructokinase muscle type; PGM1, phosphoglycerate mutase 1; PKM, pyruvate kinase muscle isozyme; G6PD, glucose-6-phosphate dehydrogenase; PKM2, pyruvate kinase M2; ATP, adenosine triphosphate; ADP, adenosine diphosphate; NADH, nicotinamide adenine dinucleotide.

Correspondence to: Yasuto Akiyama, MD, Immunotherapy Division, Shizuoka Cancer Center Research Institute, 1007 Shimonagakubo, Nagaizumi-cho, Sunto-gun, Shizuoka 411-8777, Japan. Tel: +81 559895222 Ext. 5330, Fax: +81 559896085, e-mail: y.akiyama@scchr.jp

Key Words: STAT3, shRNA, Warburg effect, cancer metabolomics, proteomics.

HIF-1α is a specific target gene for STAT3 and is closely linked to STAT3 activation (9-11). HIF-1α protein becomes stabilized under hypoxia, and contributes to the activation of glycolysis and down-regulation of mitochondrial respiration. Taken together, current evidence suggests that STAT3 is not only a constitutively activated pro-oncogenic transcription factor by virtue of its tyrosine-phosphorylation and nuclear localization, but also a mitochondria-localized metabolic regulator when serine-727 is phosphorylated.

In the present study, we found that STAT3 gene inhibition significantly suppressed the proliferation of a highly STAT3-activated lymphoma cell line, and we investigated the effect of STAT3 inhibition on metabolic switching using 2-dimensional differential gel electrophoresis (2D-DIGE) and capillary electrophoresis (CE)-time of flight (TOF)-mass spectrometry (MS) (12). With the ultimate goal of developing an efficient STAT3 inhibitor, we attempted to identify novel proteomic and metabolic biomarkers of short hairpin (sh)RNA-mediated STAT3 inhibition.

Materials and Methods

Cell lines and reagents. Human lymphoma, SCC-3 cells were supplied by the Health Science Research Resources Bank (Osaka, Japan). PANC1, MDA-MB468 and U87 cell lines were purchased from the American Type Culture Collection (Manassas, VA, USA). A highly metastatic derivative of the MKN45 gastric cancer cell line, MKN45P, was described previously (13). Cell lines were cultured in RPMI-1640 or Dulbecco's modified Eagle's medium (DMEM) (Sigma-Aldrich, St. Louis, MO, USA) supplemented with L-glutamine (2 mM), penicillin (100 U/ml), streptomycin (100 U/ml) and 10% (v/v) fetal bovine serum (FBS, Gibco, Paisley, UK). Antibodies against STAT3, phosphoSTAT3 (Tyr705) and β-actin were purchased from Cell Signaling Technology, Inc. (Danvers, MA, USA) and Becton-Dickinson (BD) Biosciences (Franklin Lakes, NJ, USA) for western blotting.

Inhibition of STAT3 gene expression using shRNA transduction. STAT3 shRNA was transduced into SCC-3 cells by electroporation using Nucleofector II (Amaxa Biosystems GmbH, Cologne, Germany). Four micrograms of plasmid at 1 mg/ml containing STAT3 shRNA (SureSilencing shRNA vector; Qiagen GmbH, Hilden, Germany) was suspended in 100 μl of solution C (VCA-1004) and added to 1-2×10^6 SCC-3 cells. After electroporation *via* program W-01, SCC-3 cells transduced with STAT3 shRNA were maintained in RPMI1640 medium containing 10% FBS and hygromycin (Life Technology, Carlsbad, CA, USA) with increasing dose up to 800 μg/ml. SCC-3 cells transduced with mock or STAT3 shRNA-4 were cultured for more than one month, and used for proteomic and metabolomic analyses. In a similar method, PANC1, NKN45P, MDA-MB468 and U87 cells were transduced with mock or STAT3 shRNA, and then the inhibitory effect on cell proliferation was investigated in each cell line.

Cell proliferation assay. Cell proliferation was examined using the WST-1 assay (Dojin Kagaku Corp., Kumamoto, Japan). Briefly, 1×10^4 cells transduced with mock shRNA, STAT3 shRNA-3 or shRNA-4 were seeded into each well of a 96-well microculture plate (Corning, NY, USA). After three days, WST-1 substrate was added to the culture, and the optical density (OD) was measured at 450 and 620 nm using an immunoreader (Immuno Mini NJ-2300, Nalge Nunc International, Roskilde, Denmark).

2D-DIGE. The proteins from SCC-3 cells transduced with mock or STAT3 shRNA-4 were extracted and labeled with Cy dyes as reported previously (13). All samples were separated by 2D-DIGE. Briefly, one-dimensional separation was performed according to pI, and two-dimensional separation was performed using Mr. IPG strips (GE Healthcare UK Ltd., Buckinghamshire, England). The strips were rehydrated with the CyDye-labeled protein mixture for 12 h at 20˚C, and electrophoresis was performed at 30 V using the IPGphor system (GE Healthcare). After equilibration, the IPG gels were applied onto a 24 cm acrylamide gel (10-12.5%). SDS-PAGE was performed at 2.5 W/gel for 30 min and then at 30 W/gel (maximum 100 W) for 4-5 h at 15˚C. Labeled sample gels were scanned at the appropriate wavelengths for Cy2, Cy3 and Cy5 using a Typhoon 9410 instrument (GE Healthcare).

The spots were detected and quantified with DeCyder software in the DIA mode (GE Healthcare). Only those spots greater than 1.5-fold changes in volume after normalization between mock and STAT3 shRNA-4 samples were defined as spots of interest. Purified peptides from trypsin-digested gels were analyzed by matrix-assisted laser desorption ionization-time of flight mass spectrometry using a 4700 proteomics analyzer (Applied Biosystems, Foster, CA, USA). Ions specific for each sample were then used to interrogate human sequences entered in the NCBInr database using the MASCOT (www.matrixscience.com) database search algorithms.

Capillary electrophoresis-time of flight-mass spectrometry (CE-TOF-MS). SCC-3 cells at 80% confluence were transduced with mock or STAT3 shRNA-4 in 10-cm^2 culture dishes; they were then quenched using LC-MS-grade methanol and harvested. Intracellular metabolites were extracted as described previously (14). Briefly, cellular metabolites were extracted using two-phase liquid extraction. Methanol, chloroform, and water were mixed in a 10:10:4 volume ratio. The aqueous phase was finally collected for extraction of water-soluble low-molecular-weight metabolites and centrifugally filtered. After the removal of the solvent using a vacuum concentrator, the residue was dissolved in 50 μL of Milli-Q water and subjected to CE-TOF-MS analysis. All CE-TOF-MS experiments were performed using the Agilent Capillary Electrophoresis system equipped with an Agilent 6224 TOF-MS, Agilent 1200 isocratic HPLC pump, Agilent G1603 CE-MS adapter kit, and Agilent G1607 CE-electrospray ionization-MS sprayer kit (Agilent Technologies, Santa Clara, CA, USA) as described previously (14). For system control and data acquisition, G2201AA ChemStation software was used for CE and MassHunter software was used for TOF-MS (Agilent Technologies). Metabolites were quantitatively identified using metabolomics analysis software for alignment and annotation, MasterHands (Keio University, Tsuruoka, Japan), based on the m/z (calculated exact mass) and the migration time of the reference metabolite materials.

Quantitative polymerase chain reaction (qPCR) analysis. The real-time PCR analysis of 2D-DIGE-identified (proteomic) marker genes and metabolic enzyme genes involved in glycolysis was performed using the 7500 Real Time PCR System (Applied Biosystems) as

described previously (15). Briefly, all PCR primers [adenosine triphosphate (ATP)5B, latexin (LXN), SERPINB4, 15-hydroxyprostaglandin dehydrogenase (15-HPGD), and fructose-bis-phosphate aldolase A (ALDOA) as proteomic markers; hexokinase 2 (HK2), 6-phosphofructo-2-kinase/fructose-2,6-bisphosphatase 3 (PFKFB3), phosphofructokinase (PFKM), phosphoglycerate mutase 1 (PGM1), pyruvate kinase muscle isozyme (PKM), and pyruvate dehydrogenase kinase 1 (PDK1) as metabolic enzyme genes] and TaqMan probes were purchased from Applied Biosystems. Total RNAs from SCC-3 cells transduced with mock or STAT3 shRNA-4 and *in vivo* SCC-3 tumors were extracted. SCC tumors were harvested from tumor-bearing nude mice treated with STAT3 inhibitor, STX-0119 for five days, which was described previously (16) and isolated RNAs were used for a real-time PCR analysis of latexin gene. Complementary DNA was synthesized from 100 ng of the total RNA, and quantitative PCR was carried-out using a TaqMan RNA-to-Ct 1-Step kit (Applied Biosystems).

Western blotting. A total of 5×10^6 SCC-3 cells transduced with mock or STAT3 shRNA-4 were lysed using RIPA buffer (Thermo Fisher Scientific Inc., Rockford, IL, USA) containing protease inhibitors and phosphatase inhibitors and used for western blotting as described previously (13). Briefly, cell lysates were subjected to SDS-PAGE on a 7.5% polyacrylamide separating gel, and then transferred to membranes. After blocking, the membranes were incubated at 4˚C overnight with primary antibodies against STAT3, phosphoSTAT3 and β-actin in blocking solution. After a wash, the membranes were incubated for 1 h with horseradish peroxidase-conjugated anti-mouse IgG. The membranes were treated with ECL plus reagent (GE Healthcare) and analyzed on a chemiluminescence scanner (LAS-3000, FUJIFILM, Tokyo, Japan).

Animal experiments. Male nude mice (BALB/cA-nu/nu, 5-6 weeks old) were obtained from Nippon Clea (Tokyo, Japan). All animals were cared for and used humanely according to guidelines for the Welfare and Use of Animals in Cancer Research published in Br J Cancer in 2010 (17), and the procedures were approved by the Animal Care and Use Committee of Shizuoka Cancer Center Research Institute (Approved No.25-5). SCC-3 cells transduced with mock shRNA or STAT3 shRNA-3 or shRNA-4 were re-suspended in RPMI-1640 medium (100μl) containing Matrigel (BD Biosciences) at 1×10^7/mL, and inoculated into the flank of five BALB/cA-nu/nu mice per group. Tumor volumes were calculated based on the National Cancer Institute formula as follows: tumor volume (mm^3) =length (mm) × [width (mm)]^2 × 1/2.

Statistical analysis. Significant differences were analyzed using Student's paired two-tailed *t*-test. Values of $p<0.05$ were considered significant.

Results

Inhibitory effect of STAT3 shRNA on the proliferation of SCC-3 cells. STAT3 protein expression and STAT3 phosphorylation were both inhibited by approximately 70% in STAT3 shRNA-4 transduced-SCC-3 cells (Figure 1A and B). Additionally, the STAT3 target genes c-MYC, cyclin D1, and survivin were down-regulated in shRNA-treated cells compared to those treated with mock shRNA. STAT3 gene inhibition by shRNA-4 transduction significantly suppressed the proliferation of SCC-3 cells compared with mock shRNA (Figure 1C). Moreover, shRNA-4-mediated STAT3 gene inhibition had an inhibitory effect even on *in vivo* transplanted tumor (Figure 1D and E). In STAT3 shRNA-4-transduced SCC-3 tumor, approximately 50% reduction of tumor growth was recognized compared to tumor with mock gene transduction.

2D-DIGE. Two 2D-DIGE experiments were performed, and five gels were utilized for image matching in each experiment. Comparing the protein spots between the Cy3-labeled mock and the Cy5-labeled shRNA group, the number of spots that changed by more than 1.5-fold was 13 out of the total 2,482 spots. A gel image in which 13 spots were selected is shown in Figure 2A, and the identified protein list is given in Table I. Five different proteins were identified, but spot 1 was not a hit in the MASCOT database search. Spot numbers 4-11 were revealed to be the same protein, ALDOA. Out of the 13 spots, two were up-regulated and 11 were down-regulated proteins. The down-regulated proteins were serpin B4, ALDOA and 15-HPGD. The up-regulated proteins were ATP synthase subunit-β (ATP5B) and latexin.

Proteomic marker expression using real-time PCR analysis. *ATP5B* and *latexin* mRNA were up-regulated, and mRNA for *ALDOA*, *15-HPGD* and *serpin B4* was found down-regulated, which was in accordance with the 2D-DIGE analysis. In particular, the fold changes of 15-HPGD and latexin were the highest, at approximately 4.0 (Figure 2B).

CE-TOF-MS. Metabolic pathways in cancer cells and the involvement of key enzymes are shown in Figure 3A. Metabolites in glycolysis were mainly analyzed using CE-TOF-MS in STAT3-knockdown SCC-3 cells. Eight metabolites and associated molecules including glucose-6-phosphate (G6P), fructose-6-phosphate (F6P), fructose-1,6-bisphosphate (F6BP), 3-phosphoglyceric acid (3-PGA), alanine, lactate, nicotinamide adenine dinucleotide (NADH)/NAD^+, and ATP/adenosine diphosphate (ADP) were quantitatively analyzed (Figure 3B). As a result, G6P, F6P, F6BP, and the ATP/ADP ratio were shown to decrease in STAT3 shRNA-treated cells. In contrast, alanine and lactate increased in shRNA-treated cells.

Metabolic enzyme gene expression using real-time PCR analysis. The expression levels of metabolic enzyme genes involved in the glycolysis pathway shown in Figure 3A were analyzed using quantitative PCR. PFKFB3, PFKM, PGM1 and PKM were down-regulated in STAT3-knockdown SCC cells (Figure 3C). By contrast, HK2 and PDK1 were not inhibited by shRNA-mediated STAT3 inhibition. Additionally, using four cancer cell lines with STAT3 signal activation such as PANC1,

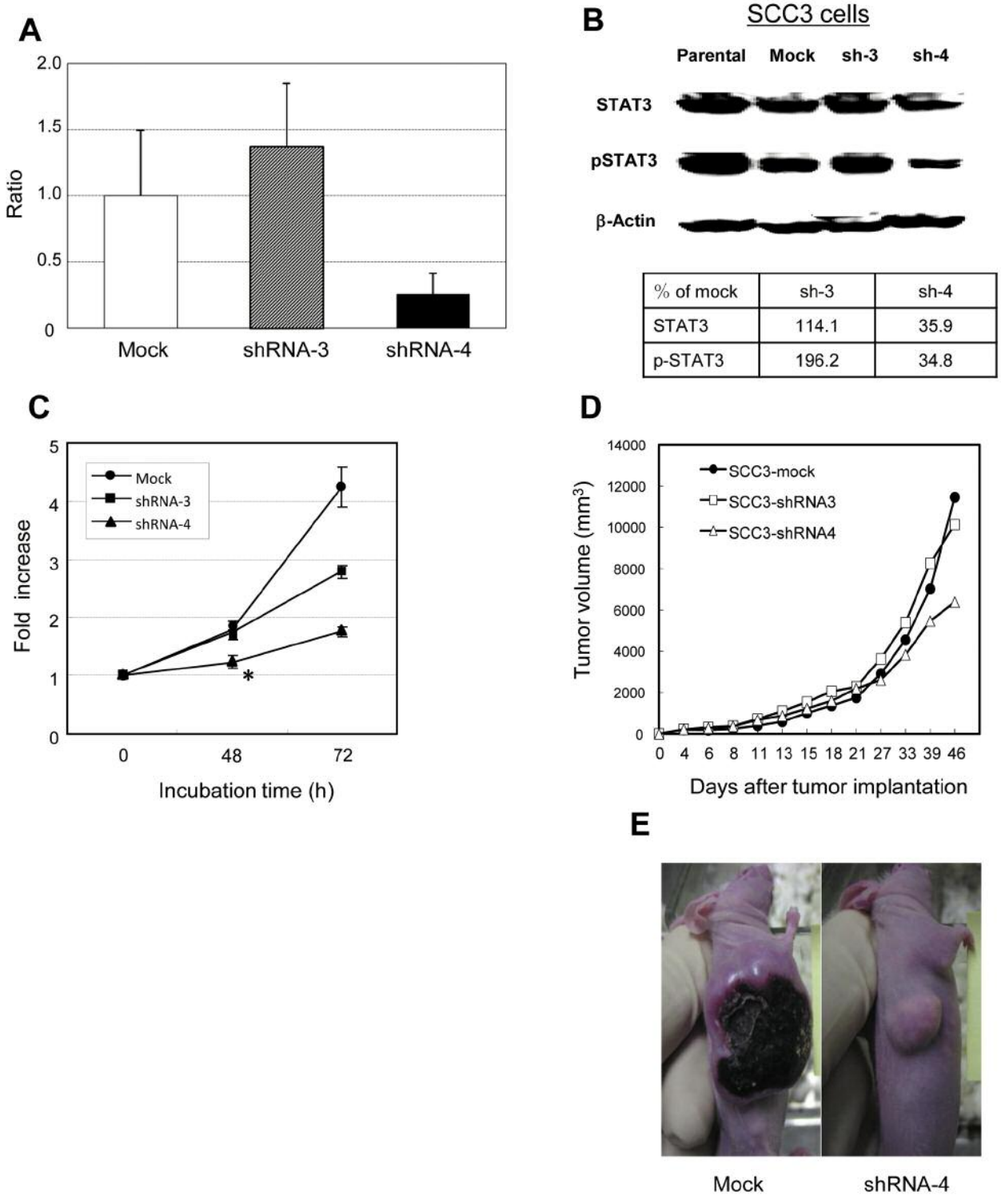

% of mock	sh-3	sh-4
STAT3	114.1	35.9
p-STAT3	196.2	34.8

Figure 1. *Inhibitory effect of shRNA-mediated STAT3 inhibition on the cell proliferation and tumor growth of SCC-3 cells. A: Inhibition of STAT3 mRNA in STAT3-specific shRNA-4-transfected SCC-3 cells according to real-time PCR. Each column shows the mean±SD of quadruplicate samples. B: Suppression of STAT3 protein by 70% in shRNA-4-transfected SCC-3 cells according to western blot assay. C: Proliferation of the shRNA-transduced SCC-3 cell line. ● Mock, ■ STAT3 shRNA-3, ▲ STAT3 shRNA-4. Each point shows the mean value of triplicate samples. *p<0.05, statistically significant compared to mock. D: Tumor growth of the shRNA-transduced SCC-3 cell line in vivo. ● Mock, □ STAT3 shRNA-3, △ STAT3 shRNA-4. Each point shows the mean value of five mice. E: Images of SCC-3 tumors transfected with mock or STAT3 shRNA-4 on day 46 after implantation.*

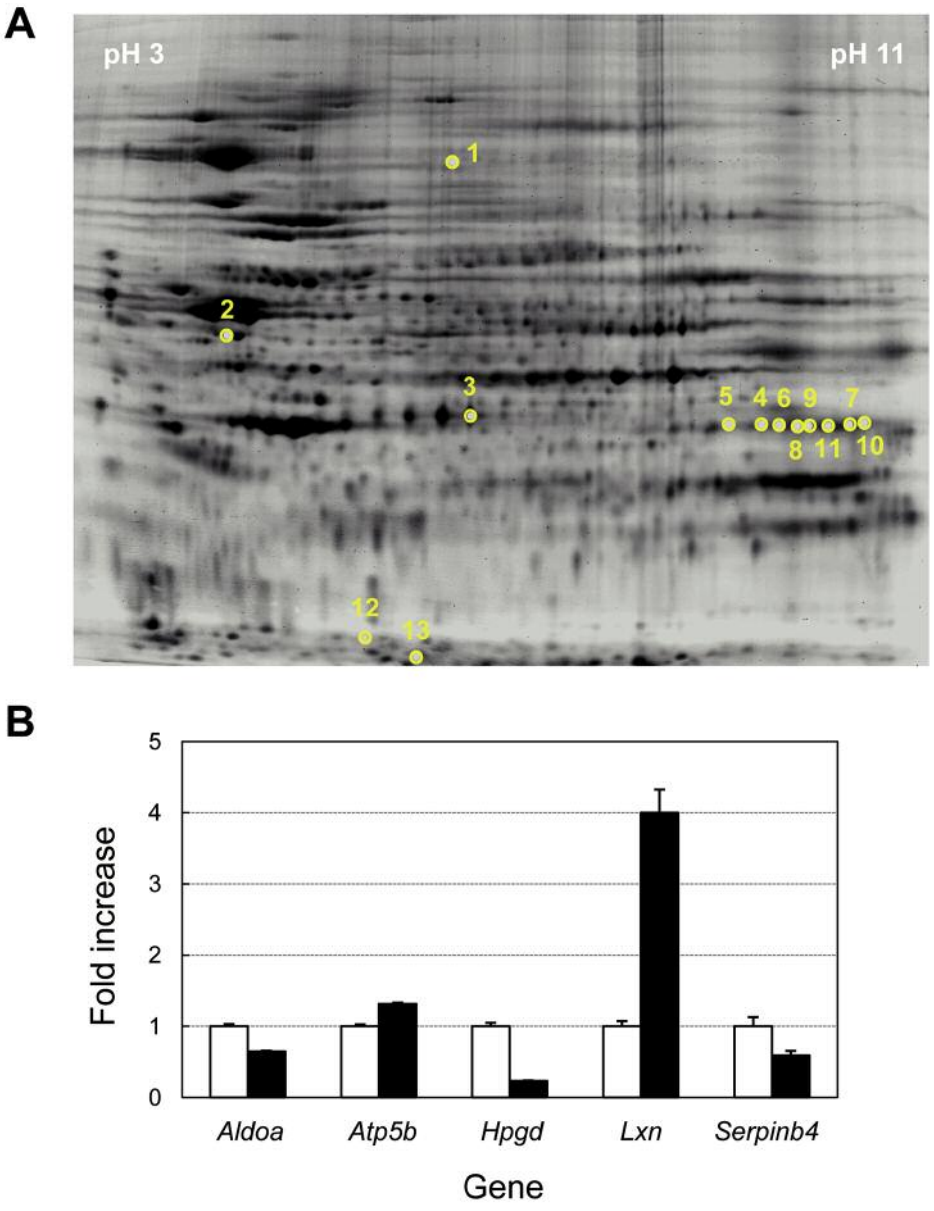

Figure 2. *Characterization of proteomic markers identified in 2D-DIGE. A: 2D-DIGE using SCC-3 cells transfected with mock or STAT3 shRNA was performed. Comparing the protein spots between the Cy3-labeled mock and the Cy5-labeled shRNA-4 group, 13 spots were changed by more than 1.5-fold. The list of identified proteins is shown in Table I. B: Changes in mRNA expression for proteomic markers identified in 2D-DIGE. The expression of ATP5B, LXN, SERPINB4, 15-HPGD, ALDOA was evaluated using real-time PCR. The expression level of each gene in the mock-transfected SCC-3 cells was rated as 1. Each point shows the mean value for quadruplicate samples.*

NKN45P, MDA-MB468 and U87 cells which were transduced with STAT3 shRNA, metabolic enzyme levels were analyzed. PDK1, PFKFB3, PGM1 and PKM were down-regulated in more than two cell lines as in SCC-3 cells (Table II).

Restoration of latexin mRNA expression in STAT3-knockdown cancer cells other than SCC-3 cells. Five cancer cell lines, including SCC-3 cells, that showed activation of STAT3 signaling, were transduced with STAT3-specific shRNA. The expression of STAT3 in all cell lines was inhibited by more than 60% and cell proliferation of shRNA-transduced cells was also significantly inhibited. Additionally, the growth of tumors was suppressed in four cell lines transduced with STAT3 shRNA (Figure 4A). Meanwhile, *latexin* mRNA expression was restored after shRNA-mediated STAT3 inhibition in three cancer cell lines (Figure 4B). In particular, latexin expression was up-

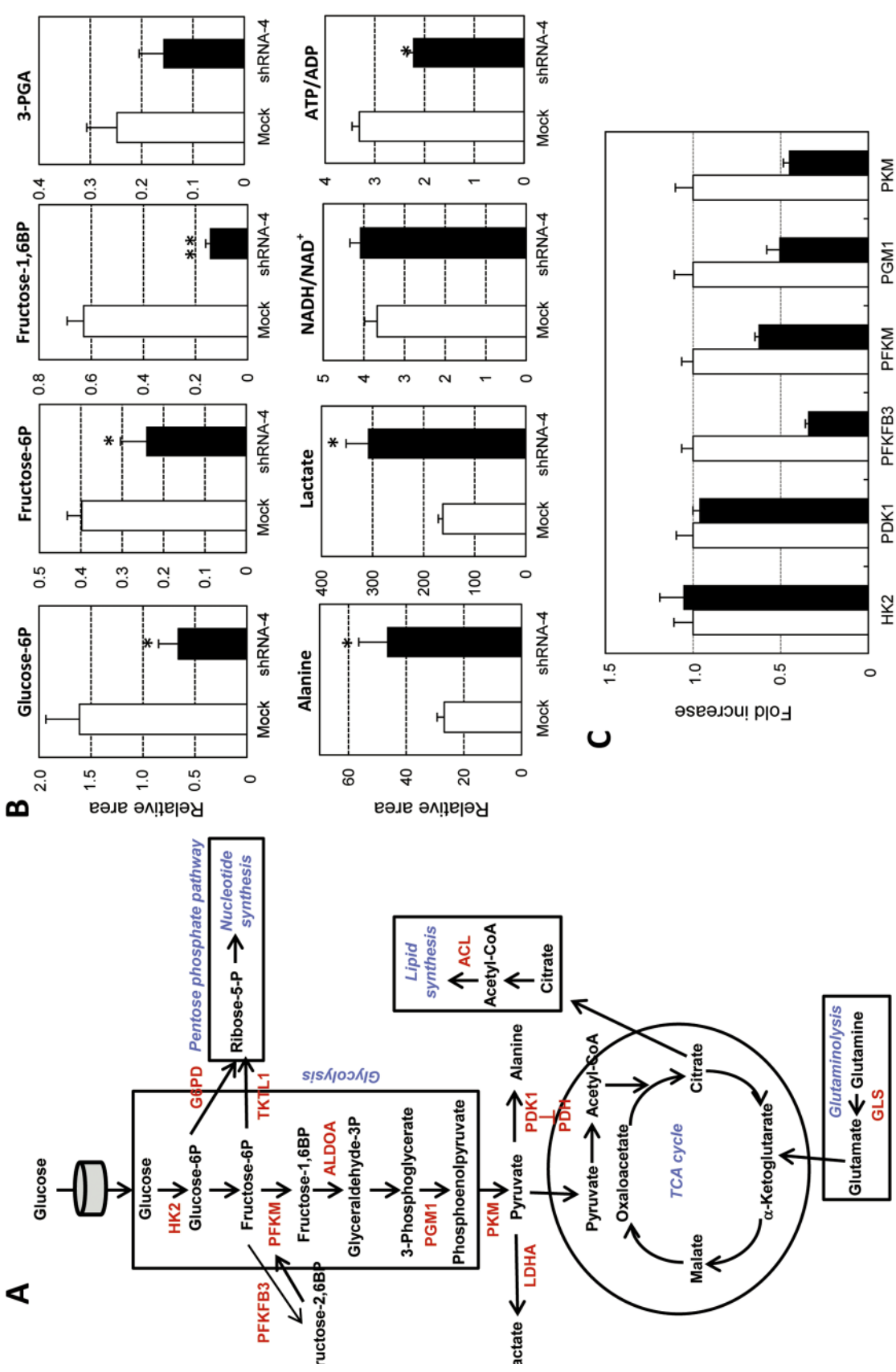

Figure 3. *Metabolic changes induced by shRNA-mediated STAT3 gene inhibition in a highly STAT3-activated SCC cell line. A: Metabolic pathway of cancer cells. The metabolic pathway and key enzymes of glycolysis, the TCA cycle, the pentose phosphate pathway, glutaminolysis and lipid synthesis are shown. B: Metabolites in STAT3 gene-knockdown SCC-3 cells were analyzed using CE-TOF-MS. Eight parameters, including G6P, F6P, F6BP, 3-PGA, alanine, lactate, the NADH/NAD+ ratio and the ATP/ADP ratio, were measured. Each column shows the mean of four determinations. *p<0.05, statistically significant compared to mock. C: Expression of key metabolic enzyme in SCC-3 cells transfected with STAT3 shRNA. The expression of HK2, PFKM, PGM1, PFKFB3, PKM, and PDK1 was measured using real-time PCR. The expression level of each gene in the mock-transfected SCC-3 cells was rated as 1. Each point shows the mean value for quadruplicate samples.*

Table I. *Proteins identified using STAT3 gene-inhibited SCC-3 cells.*

No.	Protein name	Ratio	Score	Mr	pI
1	-	−1.84	-	-	-
2	ATP synthase subunit beta	1.72	287	56525	5.26
3	Serpin B4	−1.51	482	44825	5.86
4	Fructose-bisphosphate aldolase A	−1.76	207	39395	8.30
5	Fructose-bisphosphate aldolase A	−1.51	20	39395	8.30
6	Fructose-bisphosphate aldolase A	−1.64	189	39395	8.30
7	Fructose-bisphosphate aldolase A	−1.62	271	39395	8.30
8	Fructose-bisphosphate aldolase A	−1.58	245	39395	8.30
9	Fructose-bisphosphate aldolase A	−1.6	147	39395	8.30
10	Fructose-bisphosphate aldolase A	−1.67	239	39395	8.30
11	Fructose-bisphosphate aldolase A	−1.58	365	39395	8.30
12	Latexin	2.18	114	25734	5.54
13	15-Hydroxyprostaglandin dehydrogenase	−2.15	271	28959	5.5

Numbers (No.) in the table correspond with spot numbers shown in Figure 2. The ratio is the a fold change of protein spot volume between mock and shRNA-4-transfected SCC-3 cells. Plus and minus values indicate up-regulation and down-regulation of protein expression in STAT3 shRNA-transfected compared with mock-transfected cells, respectively.

Table II. *Effect of STAT3 inhibition on the relative expression of metabolic enzymes. The expression of metabolic enzymes in STAT3 gene-inhibited cells was measured using real-time PCR. The expression level of each gene in the mock-transfected SCC-3 cells was rated as 1.*

Cell line	HK2	PDK1	PFKFB3	PFKM	PGM1	PKM	TKTL1
SCC-3	1.06±0.06	0.96±0.03	0.34±0.01**	0.63±0.02**	0.51±0.03**	0.45±0.02**	ND
MKN45P	0.78±0.05**	1.04±0.05	1.31±0.06	1.02±0.05	1.27±0.11	1.24±0.07**	2.75±0.19
PANC1	1.02±0.05	0.85±0.04**	0.53±0.03**	0.87±0.04*	0.63±0.03*	0.70±0.04**	0.29±0.02**
U87	0.71±0.06*	0.72±0.04*	0.85±0.06*	1.47±0.10	1.17±0.07	1.03±0.10	0.84±0.17
MDA-MB468	1.00±0.0	0.69±0.02**	1.19±0.05	1.36±0.05	0.74±0.03**	1.39±0.06	ND
SEKI	1.62±0.14	0.95±0.06	1.48±0.06	1.60±0.08	1.51±0.06	1.03±0.05	4.57±0.45

Data are the mean of quadruplicate samples. Significantly different at *$p<0.05$ and **$p<0.01$ from mock-transfected cells. ND: Not done.

regulated more than 8-fold after STAT3 knockdown in U87 cells. More importantly, the up-regulation of *latexin* mRNA expression was also identified *in vivo* tumors transplanted to nude mice which were treated STAT3 inhibitor, STX-0119 for five days compared with the control group without treatment (Figure 4C).

Discussion

ATP, required by proliferating cells, is derived from two main sources. One is glycolysis, which metabolizes glucose to pyruvate in the cytoplasm, producing two molecules of ATP per molecule of glucose. The other is the tricarboxylic acid (TCA) cycle, which uses pyruvate and supplies electrons to the respiratory chain complexes in the mitochondria, in which 36 molecules of ATP per molecule of glucose are produced. Cancer cells consume a substantial amount of glucose and produce lactate for ATP production. The shift towards lactate production in cancer cells, even in a non-hypoxic environment, is termed the Warburg effect (5, 6). Cancer tissues perform aerobic glycolysis through activation of oncogenes or loss of tumor suppressor proteins, which is highly promoted by the stabilization of HIF proteins. Recent advances of multiomics-based analyses have enabled us to clarify part of the mechanism responsible for the Warburg effect in cancer cells (18-20), which has contributed to the development of novel therapeutic approaches targeting cancer cell dependence on glycolysis and ATP citrate lyase (21-23).

We previously reported that a human lymphoma cell line, SCC-3 exhibits constitutively high STAT3 activation (16). We demonstrated that specific STAT3 knockdown by shRNA inhibited the growth of SCC-3 cells *in vitro* and *in vivo*. In the present study, we dissected the mechanism responsible for the growth inhibition and searched for novel biomarkers reflecting STAT3 inhibition-mediated growth suppression of SCC-3 cells using 2D-DIGE and CE-TOF-MS.

2D-DIGE analysis revealed five proteins as being differentially expressed: ATP synthase and latexin were up-regulated, and ALDOA, serpin B4 and 15-PGDH were down-regulated. ATP synthase, especially the ectopic ATP synthase subunit, is expressed on the membrane surface of the non-

A

	Cell line (shRNA)				
	SCC-3	PANC1	MKN45P	MDA-MB 468	U87
STAT3 Inhibition (%)	74	72	70	60	60
Inhibition of cell proliferation	+	+	+	+	+
Inhibition of tumor growth	+	+	+	+	ND

B

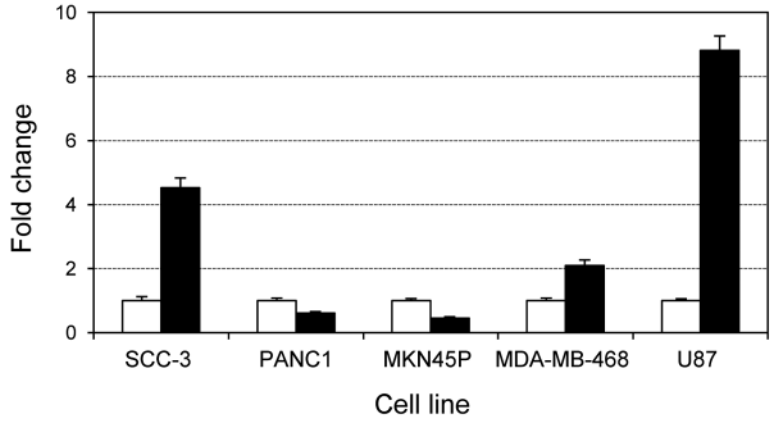

C

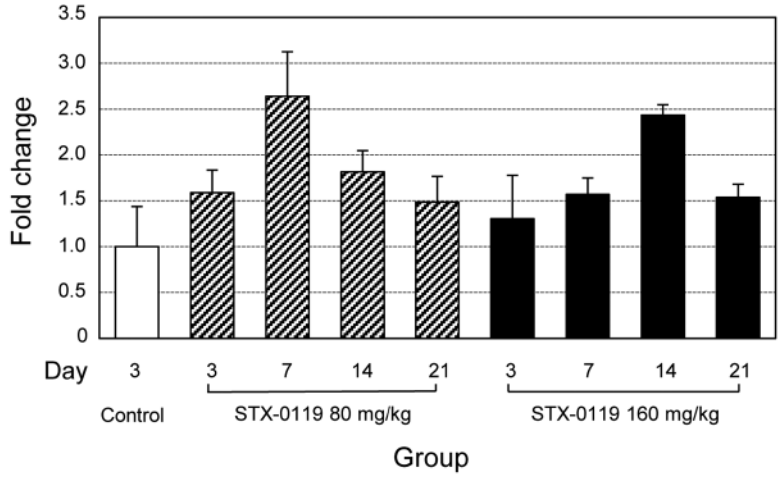

Figure 4. *Restoration of latexin mRNA expression in STAT3 knockdown in cancer cell lines using a real-time PCR. A: STAT3 inhibition by shRNA and its effect on cancer cell proliferation and tumor growth in vivo in five cancer cell lines including SCC-3. B: The restoration of latexin mRNA expression after STAT3 gene inhibition. Open column: mock shRNA, closed column: STAT3 shRNA. The expression level of each gene in the mock-transfected cells was rated as 1. C: The up-regulation of latexin mRNA in SCC-3 tumors transplanted to node mice treated with STX-0119 administered on days 1 to 5. The tumors were harvested on days 3, 7, 14 and 21. The expression level of the control tumor harvested on day 3 was rated as 1. Each column shows the mean value for quadruplicate samples.*

small cell lung cancer cell line A549 (24), and it is a potential cancer-specific biomarker associated with metastasis (25) and a therapeutic target for developing ATP synthase inhibitors (26). Our study did not show any reduction of ATP synthase in STAT3-inhibited cells, but STAT3 inhibition does inhibit ATP production by suppressing mitochondrial function (27, 28), which might be partly in accordance with our observation of a reduction of the ATP/ADP ratio.

ALDOA cleaves fructose-1,6BP to glyceraldehyde-3 phosphate, which is finally metabolized to pyruvate by way of 3-phosphoglycerate and phosphoenolpyruvate in the glycolysis pathway. This pathway should promote an increase of ATP production in the anaerobic state in cancer cells (29). Here, all investigated metabolic genes contribute to the metabolism of fructose-6P to pyruvate (PFKFB3, PFKM, ALDOA, PGM1 and PKM), were down-regulated. In particular, ALDOA was strongly down-regulated, even at the protein level. These results might suggest that suppression of glycolytic activation in cancer cells can be mediated by inhibition of STAT3 signaling.

Latexin acts as a tumor suppressor and hematopoietic stem cell-regulating protein, and its expression is reduced in human gastric cancer and lymphoma (30-32). In our study, latexin expression was up-regulated in three cancer cell lines, aside from SCC-3 transduced with STAT3-specific shRNA. Impressively, the up-regulation of latexin expression was identified in SCC-3 tumors transplanted to nude mice after the treatment by STAT3 inhibitor. The restoration of latexin expression after STAT3 gene inhibition suggests a potential link to STAT3 signaling. However, no correlation of STAT3 with latexin has been reported. In the near future, the interaction of STAT3 with latexin methylation should be investigated.

15-PGDH is considered to play a key role as a tumor suppressor in gastrointestinal cancers. Ryu *et al*. (33) demonstrated that 15-PGDH expression is significantly reduced in *Helicobacter pylori*-positive gastric cancers, and its expression is restored after *H. pylori* eradication therapy. Meanwhile, STAT3 and cyclo-oxygenase (COX)2 are closely linked key molecules in triggering long-term inflammation and contribute to an environment conductive to carcinogenesis. Specifically, the knockdown of STAT3 attenuates COX2 expression in gastric cancer cell lines (34). Interestingly, the COX2-specific inhibitor celecoxib (35) significantly reduces STAT3 phosphorylation and down-regulates STAT3 target genes including BCL-2, survivin and cyclin D1. 15-PGDH, as a tumor suppressor, and STAT3 and COX2, as pro-tumor factors, have opposing actions in cancer cell-associated signaling pathways.

Cancer cells continue to exhibit high ratios of ATP/ADP and $NADH/NAD^+$ due to the alternative mode of ATP production of converting two ADPs to one ATP and one AMP catalyzed by adenylate kinases (3). This helps not only to maintain a viable ATP/ADP ratio but also to accumulate AMP, which can lead to the phosphorylation of other target proteins to improve the energy charge in the proliferating cells. In our study, shRNA-mediated STAT3 inactivation reversed the glycolytic shift by reducing metabolic enzyme genes such as ALDOA and fructose-1,6-BP and by reducing the ATP/ADP ratio.

Recently, Demaria *et al*. demonstrated a potential correlation of STAT3 with the Warburg effect, in a metabolomics analysis (10), which indicates that activated STAT3 acts as a master regulator of cell metabolism by inducing both aerobic glycolysis and down-regulation of mitochondrial activity. In particular, STAT3-mediated up-regulation of HIF-1α is considered an additional important factor that promotes glycolysis and mitochondrial suppression in cancer cells. Additionally, our finding that STAT3 inhibition in highly STAT3-activated cancer cells induced not only growth suppression but also the restoration of the metabolic shift to glycolysis, suggests that the induction of aerobic glycolysis is an important biological aspect of the pro-oncogenic activities of STAT3. Therefore, metabolic markers closely linked to STAT3 signaling are potential novel targets associated with the metabolic shift in cancer and could be used to develop a new type of STAT3 inhibitor regulating serine-727 phosphorylation-associated STAT3 localization to mitochondria.

In the current study, we identified latexin as a proteomic marker candidate and metabolic enzymes such as ALDOA and fructose-1,6DP as candidate metabolic markers for STAT3-targeting therapy using our STAT3-specific shRNA gene transduction model. Our observations could contribute to the development of new inhibitors of STAT3 signaling for cancer treatment in the near future.

Conflicts of Interest

The Authors have no conflicts of interest.

Acknowledgements

This work was supported by a grant from the regional innovation strategy support program of the Ministry of Education, Culture, Sports, Science and Technology, Japan

References

1 Zhong Z, Wen L and Darnell JE Jr.: Stat3: a STAT family member activated by tyrosine phosphorylation in response to epidermal growth factor and interleukin-6. Science *264*: 95-98, 1994.
2 Bromberg J and Darnell JE Jr.: The role of STATs in transcriptional control and their impact on cellular functions. Oncogene *19*: 2468-2473, 2000.
3 DeBerardinis RJ, Lum JJ, Hatzivassiliou G and Thompson CB: The biology of cancer: metabolic reprogramming fuels cell growth and proliferation. Cell Metab *7*: 11-20, 2008.
4 Marie SK and Shinjo SM: Metabolism and brain cancer. Clinics *66*: 33-43, 2011.
5 Kim JW and Dang CV: Cancer's molecular sweet tooth and the Warburg effect. Cancer Res *66*: 8927-8930, 2006.
6 Ward PS and Thompson CB: Metabolic reprogramming: a cancer hallmark even Warburg did not anticipate. Cancer Cell *21*: 297-308, 2012.
7 Gough DJ, Corlett A, Schlessinger K, Wegrzyn J, Larner AC and Levy DE: Mitochondrial STAT3 supports RAS-dependent oncogenic transformation. Science *324*: 1713-1716, 2009.

8 Wegrzyn J, Potla R, Chwae YJ, Sepuri NB, Zhang Q, Koeck T, Derecka M, Szczepanek K, Szelag M, Gornicka A, Moh A, Moghaddas S, Chen Q, Bobbili S, Cichy J, Dulak J, Baker DP, Wojfman A, Stuehr D, Hassan MO, Fu XY, Avadhani N, Drake JI, Fawcett P, Lesnefsky EJ and Larner AC: Function of mitochondrial Stat3 in cellular respiration. Science *323*: 793-797, 2009.

9 Darnell JE Jr: STAT3, HIF1, glucose addiction and Warburg effect. Aging *2*: 890-891, 2010.

10 Demaria M, Giorgi C, Lebiedzinska M, Esposito G, D'Angeli A, Bartoli A, Gough DJ, Turkson J, Levy DE, Watson CJ, Wieckowski MR, Provero P, Pinton P and Poli V: A STAT3-mediated metaboloc switch is involved in tumor transformation and STAT3 addiction. Aging *2*: 823-842, 2010.

11 Liu Q, Wang L, Wang Z, Yang Y, Tian J, Liu G, Guan D, Cao X, Zhang Y and Hao A: GRIM-19 opposes reprogramming of glioblastoma cell metabolism *via* HIF1α destabilization. Carcinogenesis *34*: 1728-1736, 2013.

12 Sugimoto M, Wong DT, Hirayama A, Soga T and Tomita M: Capillary electrophoresis mass spectrometry-based saliva metabolomics identified oral, breast and pancreatic cancer-specific profiles. Metabolomics *6*: 78-95, 2010.

13 Takikawa M, Akiyama Y, Maruyama K, Suzuki A, Liu F, Tai S, Ohshita C, Kawaguchi Y, Bandou E, Yonemura Y and Yamaguchi K: Proteomic analysis of a highly metastatic gastric cancer cell line using two-dimensional differential gel electrophoresis. Oncol Rep *16*: 705-711, 2006.

14 Urakami K, Zangiacomi V, Yamaguchi K and Kusuhara M: Impact of 2-deoxy-D-glucose on the target metabolome profile of a human endometrial cancer cell line. Biomed Res *34*: 221-229, 2013.

15 Akiyama Y, Komiyama M, Nakamura Y, Iizuka A, Oshita C, Kume A, Nogami H, Ashizawa T, Yoshikawa S, Kiyohara Y and Yamaguchi K: Identification of novel MAGE-A6- and MAGE-A12-derived HLA-A24-restricted cytotoxic T lymphocyte epitopes using an *in silico* peptide-docking assay. Cancer Immunol Immunother *61*: 2311-2319, 2012.

16 Ashizawa T, Miyata H, Ishii H, Oshita C, Matsuno K, Masuda Y, Furuya T, Okawara T, Otsuka M, Ogo N, Asai A and Akiyama Y: Antitumor activity of a novel small molecule STAT3 inhibitor against a human lymphoma cell line with high STAT3 activation. Int J Oncol *38*: 1245-1252, 2011.

17 Workman P, Aboagye EO, Balkwill F, Balmain A, Bruder G, Chaplin DJ, Double JA, Everitt J, Farningham DA, Glennie MJ, Kelland LR, Robinson V, Stratford IJ, Tozer GM, Watson S, Wedge SR, Eccles SA: Guidelines for the welfare and use of animals in cancer research *102*: 1555-1577, 2010.

18 Dang CV: Rethinking the Warburg effect with Myc micromanaging glutamine metabolism. Cancer Res *70*: 859-862, 2010.

19 Gao P, Tchernyshyov I, Chang TC, Lee YS, Kita K, Ochi T, Zeller KI, De Marzo AM, Van Eyk JE, Mendell JT and Dang CV: c-Myc suppression of miR-23a/b enhances mitochondrial glutamine expression and glutamine metabolism. Nature *458*: 762-765, 2009.

20 Jiang S, Zhang LF, Zhang HW, Hu S, Lu MH, Liang S, Li B, Li Y, Li D, Wang ED and Liu MF: A novel miR-155/miR-143 cascade controls glycolysis by regulating hexokinase 2 in breast cancer cells. EMBO J *31*: 1985-1998, 2012.

21 Xu RH, Pelicano H, Zhou Y, Carew JS, Feng L, Bhalla KN, Keating MJ and Huang P: Inhibition of glycolysis in cancer cells: a novel strategy to overcome drug resistance associated with mitochondrial respiratory defect and hypoxia. Cancer Res *65*: 613-621, 2005.

22 Hatzivassiliou G, Zhao F, Bauer D, Andreadis C, Shaw AN, Dhanak D, Hingorani SR, Tuveson DA and Thompson CB: ATP citrate lyase inhibition can suppress tumor cell growth. Cancer Cell *8*: 311-321, 2005.

23 Zaidi N, Swinnen JV and Smans K: ATP-citrate lyase: a key player in cancer metabolism. Cancer Res *72*: 3709-3714, 2012.

24 Lu ZJ, Song QF, Jiang SS, Song Q, Wang W, Zhang G, Kan B, Chen L, Yang J, Luo F, Qian ZY, Wei YQ and Gou L: Identification of ATP synthase beta subunit (ATPB) on the cell surface as a non-small cell lung cancer (NSCLC) associated antigen. BMC Cancer *9*: 16, 2009.

25 Pan J., Sun LC, Tao YF, Zhou Z, Du XL, Peng L, Feng X, Wang J, Li YP, Liu L, Wu SY, Zhang YL, Hu SY, Zhao WL, Zhu XM, Lou GL and Ni J: ATP synthase ecto-a-subunit: a novel therapeutic target for breast cancer. J Transl Med 9: 211, 2011.

26 Chang HY, Huang HC, Huang TC, Yang PC, Wang YC and Juan HF: Ectopic ATP synthase blockade suppresses lung adenocarcinoma growth by activating the unfolded protein response. Cancer Res *72*: 4696-4706, 2012.

27 Harada Y, Ishii I, Hatake K and Kasahara T: Pyvinium pamoate inhibits proliferation of myeloma/erythroleukemia cells by suppressing mitochondrial respiratory complex I and STAT3. Cancer Lett *319*: 83-88, 2912.

28 Sarafian TA, Montes C, Imura T, Qi J, Coppola G, Geschwind DH and Sofroniew MV: Disruption of astrocyte STAT3 signaling decreases mitochondrial function and increases oxidative stress in vitro. PLoS One *5*: e9532, 2010.

29 Dawson NJ, Biggar KK and Storey KB: Characterization of fructose-1,6-bisphosphate aldolase during anoxia in the tolerant turtle, Trachemys scripta elegans: an assessment of enzyme activity, expression and structure. PLoS One *8*: e68830, 2013.

30 Mitsunaga K, Kikuchi J, Wada T and Furukawa Y: Latexin regulates the abundance of multiple cellular proteins in hematopoietic stem cells. J Cell Physiol *227*: 1138-1147, 2012.

31 Li Y, Basang Z, Ding H, Lu Z, Ning T, Wei H, Cai H and Ke Y: Latexin expression is down-regulated in human gastric carcinomas and exhibits tumor supressor potential. BMC Cancer *11*: 121, 2011.

32 Liu Y, Howard D, Rector K, Swiderski C, Brandon J, Schook L, Mehta J, Bryson JS, Bondada S and Liang Y: Latexin is down-regulated in hematopietic malignancies and restoration of expression inhibits lymphoma growth. PLoS One *7*: e44979, 2012.

33 Ryu YM, Myung SJ, Park YS, Yang DH, Song HJ, Jeong JY, Lee SM, Song M, Kim do H, Lee HJ, Park SK, Fink SP, Markowitz SD, Jung KW, Kim KJ, Ye BD, Byeon JS, Jung HY, Yang SK and Kim JH: Inhibition of 15-hydroxyprostaglandin dehydrogenase by *Helicobacter pylori* in human gastric carcinogenesis. Cancer Prev Res *6*: 349-359, 2013.

34 Bai JW, Wang Z, Gui SB and Zhang YZ: Loss of 15-hydroxyprostaglandin dehydrogenase indicates a tumor-suppressor role in pituitary adenomas. Oncol Rep *28*: 714-720, 2012.

35 Liu DB, Hu GY, Long GX, Qiu H, Mei Q and Hu GQ: Celecoxib induces apoptosis and cell-cycle arrest in nasopharyngeal carcinoma cell lines *via* inhibition of STAT3 phosphorylation. Acta Pharmacol Sin *33*: 682-690, 2012.

Received March 23, 2015
Revised April 7, 2015
Accepted April 9, 2015